JTTEE5 4:25-33

Influence of Substrate Preparation on the Flattening and Cooling of Plasma-Sprayed Particles

C. Moreau, P. Gougeon, and M. Lamontagne

Impacts of plasma-sprayed molybdenum particles were monitored by detecting thermal radiation emitted by the hot particles when they flatten on the substrate surface. Evolution of the light intensity collected at two different wavelengths was used to obtain information about flattening time, flattening degree, and cooling time of the impinging particles. Variations of these parameters with substrate surface roughness were investigated on glass and molybdenum substrates. The substrate roughness significantly influenced the flattening degree and flattening time of the particles: the smoother the substrate, the larger the surface of the splats and the longer the flattening time. The cooling time, as determined from the decay time of the light signals after impact, was shorter on smooth substrates. In this case, the temperature of the splats was not radially uniform, with a lower cooling rate at the periphery.

1. Introduction

IN THE plasma spraying process, particles are accelerated and heated near their melting point by a hot plasma jet. Upon impact, these particles flatten, cool, and solidify at high speed. During the cooling process, most of the thermal energy of the impinging particles is transferred by conduction to the substrate or to previously deposited coating layers. Indeed, heat losses due to radiation and convection play only a minor role in typical conditions encountered in plasma spraying.

Understanding and describing the flattening process is difficult. During flattening, molten material flows radially at high speed while cooling and possibly solidification at the particle/substrate interface take place. Moreover, instabilities at the particle edge may occur, leading to explosion of the impinging particles. Reliable modeling of the flattening process requires knowledge of many parameters, some of which are unknown or at least not well known. Liquid viscosity, interfacial thermal resistance, wetting angle, and liquid surface energy are examples of parameters that influence the flattening and cooling of impinging particles.

In prior work, Madejski (Ref 1, 2) developed a simple analytical model depicting the flattening process of a particle, represented as a cylinder of molten material spreading on a perfectly smooth substrate. In the Madejski model, the kinetic energy of the impinging particle is transformed during particle flattening into potential surface energy and thermal energy due to friction in the viscous liquid. The thermal contact quality at the particle/substrate interface was assumed perfect. According to this model, when the surface energy and heat transfer from the particle to the substrate are neglected, the flattening ratio, d/d_0, is given by:

$$\frac{d}{d_0} = k(Re)^{0.2} = k\left(\frac{\nu \rho d_0}{\mu}\right)^{0.2}$$

where Re is the Reynolds number, d and d_0 are the final and initial diameters, respectively, of the particle, k is a constant (k = 1.2941), ν is the particle velocity before impact, ρ is particle density, and μ is the viscosity of the molten particle. More recently, different numerical models were developed for modeling the particle flattening process, leading to similar expressions for the flattening ratio of the solidified particles (Ref 3-5). Experimental verification of these relations has been carried out under different spraying conditions by measuring the final diameter of the flattened particles; relatively good agreement with the theoretical models was obtained for completely molten particles (Ref 5-7). Recently, the diameter of zirconia particles was determined by monitoring the thermal radiation emitted during particle impact on a substrate (Ref 8); good agreement was found with the model of Ref 4 and 5.

Although these studies permit better comprehension of the flattening process, the use of smooth substrates does not correspond to typical thermal spraying conditions. Indeed, the substrate surface is normally grit blasted before spraying to promote coating adhesion, which depends primarily on mechanical anchorage of the flattened particles on the substrate asperities. Thus, the first sprayed particles that impinge on the substrate hit a rough surface that considerably affects the flattening conditions. Furthermore, as the coating builds up, the impinging particles spread on already deposited layers, the roughness of which depends on the size, temperature, and velocity of the particles at impact.

Knowledge of the influence of surface roughness is important in modeling the coating formation process. Indeed, in some models, parameters such as residual stresses, thermal gradient, and porosity are computed and taken into account for each single flattened lamella (Ref 9, 10). The reliability of such models depends on a proper representation of the flattened particles after their impact on a nonideally smooth surface.

Keywords: flattening of particles, Madejski model, molybdenum particles, particle cooling, substrate roughness

C. Moreau, P. Gougeon, and **M. Lamontagne,** National Research Council Canada, Industrial Materials Institute, Boucherville, Québec, Canada J4B 6Y4

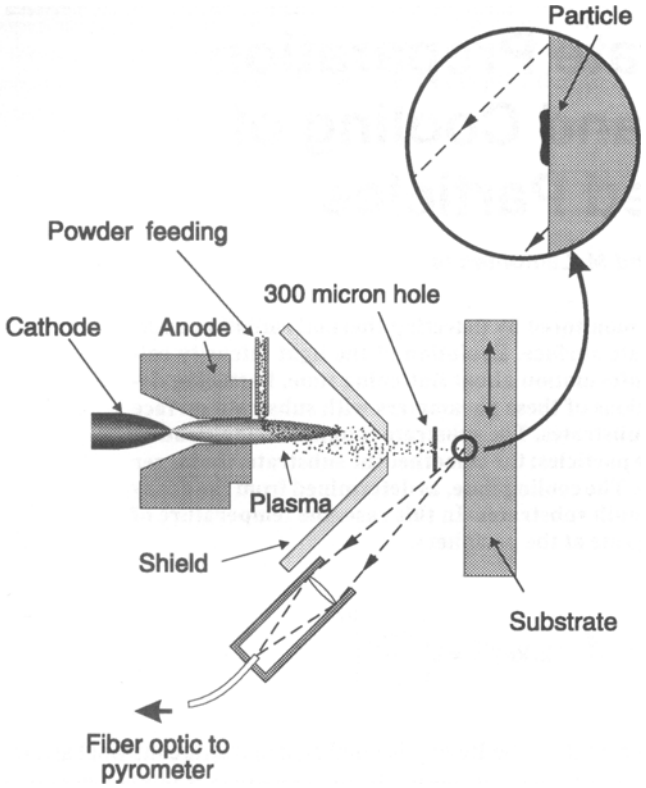

Fig. 1 Schematic of the experimental setup

A previous study (Ref 11, 12) has shown coating thickness to significantly influence the apparent flattening time and cooling time of particles upon impact. Changes noted as a function of coating thickness were attributed to changes in the nature and roughness of the surface on which the sprayed particles impacted. The goal of the present work was to clarify the specific influence of substrate roughness on the flattening of molybdenum plasma-sprayed particles. Rough glass and molybdenum substrates were grit blasted using two different grit sizes. Results obtained on these substrates were compared with those obtained on smooth substrates. Particle impact was monitored by detecting thermal radiation from the hot impinging particles through use of a fast pyrometer focused on the substrate surface.

2. Experimental

2.1 *Experimental Setup*

Figure 1 shows a schematic diagram of the experimental setup. Particles, having been heated and accelerated by the hot plasma gas, passed through two holes before hitting the substrate surface. The first hole, the nearest from the plasma torch, was 2 mm in diameter and limited the particle flux to the second hole to prevent clogging. The second hole, with a diameter of 400 μm, was located about 1.5 cm in front of the substrate surface. The thermal radiation emitted by the particles in flight and upon impact was collected by the sensor head, consisting of an achromatic lens with an optical fiber. The six-element lens was

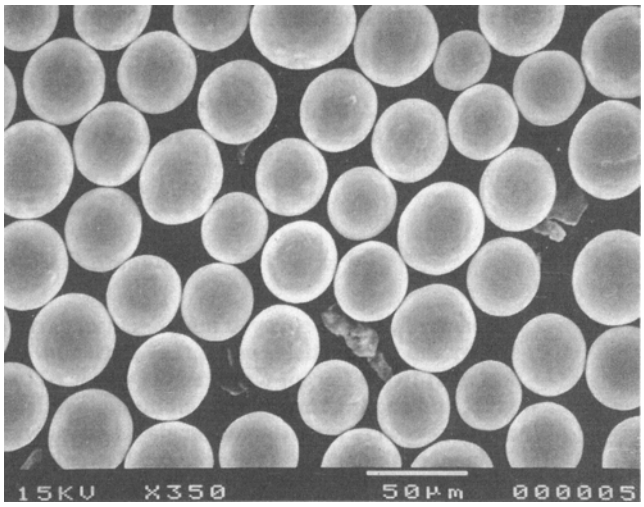

Fig. 2 Morphology of the molybdenum powder after sieving (−45+32 μm)

designed to minimize chromatic and spherical aberrations for wavelengths ranging from 700 to 1000 nm. The collected light was transmitted to a detection cabinet containing two silicon-avalanche photodetectors, D_2 and D_1, filtered at 800 and 1000 nm, respectively, by using two interference filters with bandwidths of about 50 nm. After amplification, signals from the photodetectors were digitized using a 12-bit Model 440 Nicolet oscilloscope (Nicolet Oscilloscope Div., Nicolet Instrument Corp., Madison, WI) at a sampling rate of 10 megasamples per second. The sensor head field of view on the substrate surface measured 700 by 1000 μm. The substrate, located 13 cm from the plasma torch, could be moved vertically using a precise slide and a digitally controlled direct-current motor.

2.2 *Experimental Procedure*

Measurements were carried out according to the following procedure. After reaching stable spraying conditions, the plasma torch was scanned in front of the experimental setup on a horizontal line (perpendicular to the plane of Fig. 1) in order to avoid excessive heating. During a torch passage, if a particle hit the substrate in the sensor field of view, the oscilloscope was triggered and the time evolution of the signals at both wavelengths was recorded and saved on a mass-storage magnetic disk. The trigger level was adjusted low enough so that any particle traveling in the sensor field of view could trigger the oscilloscope. After recording a particle impact, the substrate was translated by 1 mm, permitting repetition of the procedure for a new impact on a clean surface.

Plasma spraying was carried out with a Plasmasdyne SG100 (Miller Thermal, Inc., Appleton, WI) torch using the electrodes/gas injector configuration (129-145-130). The powder was injected internally in a forward direction. The arc current was 600 A, and the arc gas mixture was 50 L/min Ar and 25 L/min He. Rounded molybdenum particles were sieved to +32–45 μm to obtain a narrow particle size distribution. Figure 2 shows an electron micrograph of the sieved powder.

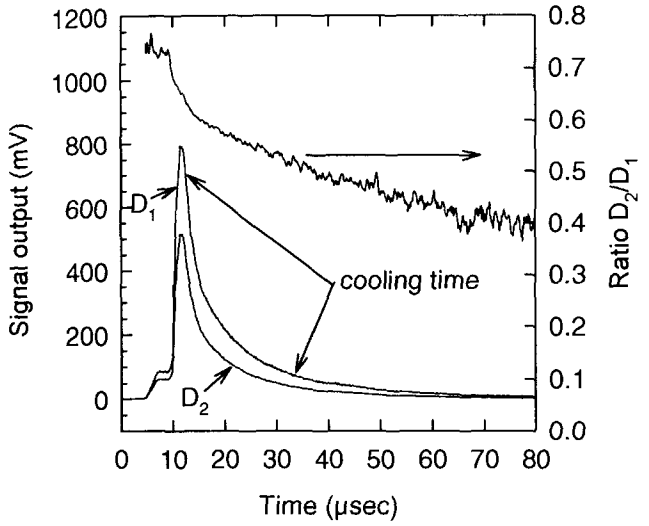

Fig. 3 Typical signals D_1 and D_2 measured during an impact on a coarse grit-blasted glass substrate. The evolution of the ratio D_2/D_1 is also shown

Grit-blasted substrates were prepared in two distinct conditions for producing two different surface roughness states. The roughest surfaces were obtained by using a National Compressed Air (National Compressed Air Canada Ltd., Mississauga, Ontario, Canada) grit-blasting machine operating at 200 kPa (30 psig) with 24-grit alumina abrasive. Fine blasting was produced using an Airbrasive 65000 System 2 (S.S. White Industrial Products, Pannwolt Corp., Piscataway, N.J.) machine operating at 530 kPa (80 psig) with 50-μm alumina grit. Surface roughness measurements (arithmetic average) were carried out using a Surtronic 3 (Taylor Hobson, Leicester, England) profilometer. Smooth glass substrates were used as received, whereas smooth molybdenum substrates were prepared by polishing with SiC papers. A final polishing with 4000-grit paper was performed on the smooth molybdenum substrate surfaces a few minutes prior to deposition to remove any oxide film.

3. Results and Discussion

3.1 *Analysis of Signals*

Figure 3 shows an example of typical signals collected when a molybdenum particle impinges on a coarse grit-blasted glass substrate. Signals D_1 and D_2 correspond to the light intensity emitted by the impinging particle at 1000 and 800 nm, respectively. At the moment of impact, the surface of the radiating particle increases rapidly, producing a rise in the signal intensity at both wavelengths (as seen at 10 μs on the time scale of Fig. 3). After reaching a maximum, the light intensity in both detectors decreases as the particle cools, its thermal energy being transferred to the substrate. The light collected before the impact, appearing as plateaus from 5 to 10 μs on the time scale of Fig. 3, comes from the in-flight particle as it travels through the pyrometer field of view and possibly from its reflection on the substrate surface. The temperature of the particle before impact can be estimated at 2850 °C from the ratio of the plateau levels after calibration of the pyrometer, assuming that the particle behaves as a gray body (Ref 13). In principle, the temperature evolution of the impinging particle can be determined from the evolution of the ratio of the detector outputs, D_2/D_1. In fact, in the present measurements, the evolution of this ratio is not fully consistent with the evolution of the intensity of thermal radiation detected at each single wavelength.

Many factors can affect the precision of the two-color pyrometer, including (1) the finite time-response of the detection system (Ref 14), (2) the deviation from gray body behavior of the radiating surface (Ref 15), (3) the detection of plasma light reflected on the substrate or particle surface (Ref 16), and (4) the presence of temperature gradients at the particle surface. These factors tend to affect the precision of two-color pyrometers more drastically than that of single-color pyrometers. In this work, the cooling time of the impacting particles is evaluated using the single-color pyrometer, D_1. Information obtained from the evolution of the ratio D_2/D_1 after particle impact is considered only on a qualitative basis. On the other hand, the temperature of the in-flight particles must be evaluated from the ratio D_2/D_1 (two-color pyrometer), because the emitting area of the particles is unknown.

As previously mentioned, the radiation collected before particle impact can be detected either directly or after reflection from the substrate surface. This is schematically illustrated in Fig. 4(a) for a particle impinging on a polished metal surface. In this case, the radiation from the in-flight particle is first collected after reflection on the substrate and, a few microseconds later, directly by the sensor head. The corresponding signals are shown in Fig. 4(b). It is worth noting that, due to diffuse reflection, radiation from the impinging particles can be detected even when the particles are relatively far from the surface of a rough substrate. On the other hand, the influence of light reflection is minimal on glass substrates, because the reflectivity of this material is low in the spectral ranges used in this study.

Information about flattening time, cooling time, and flattening degree are obtained from signal D_1, collected during the formation of individual splats. The flattening time is taken as the time lapse between the rapid signal increase corresponding to particle contact with the substrate and the occurrence of the maximum signal intensity. The cooling time is estimated by measuring the time required for the signal to decrease from 90 to 10% of its maximum value. Finally, an indication of the flattening degree is obtained by comparing the maximum value of the signal after impact with the signal level collected from the in-flight particles when they impinge on a smooth glass substrate. Indeed, in this case, reflection of the thermal radiation on the substrate surface is minimal. It should be noted that the real flattening time and flattening degree might be larger than those determined as above if significant cooling occurs during the flattening process (Ref 12). Similarly, the flattening process can influence determination of the cooling time, particularly if the particle can shrink under the influence of its surface tension before freezing (Ref 17).

3.2 *Impacts on Glass*

Figure 5 shows the results obtained on the glass substrates. The error bars correspond to one standard deviation. The surface roughness, R_a varies from 9.6 μm on the coarse grit-blasted sub-

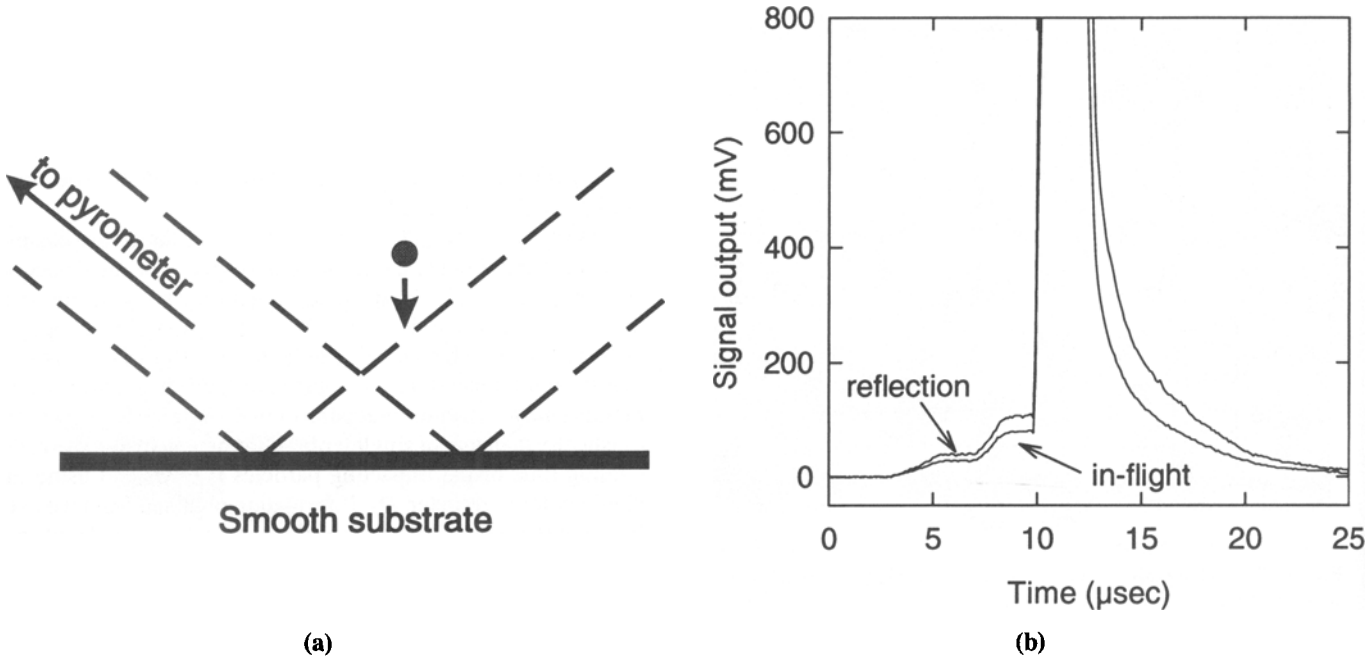

Fig. 4 (a) Schematic of an in-flight particle immediately before impact on a smooth reflecting substrate. (b) Corresponding signals collected before and during impact

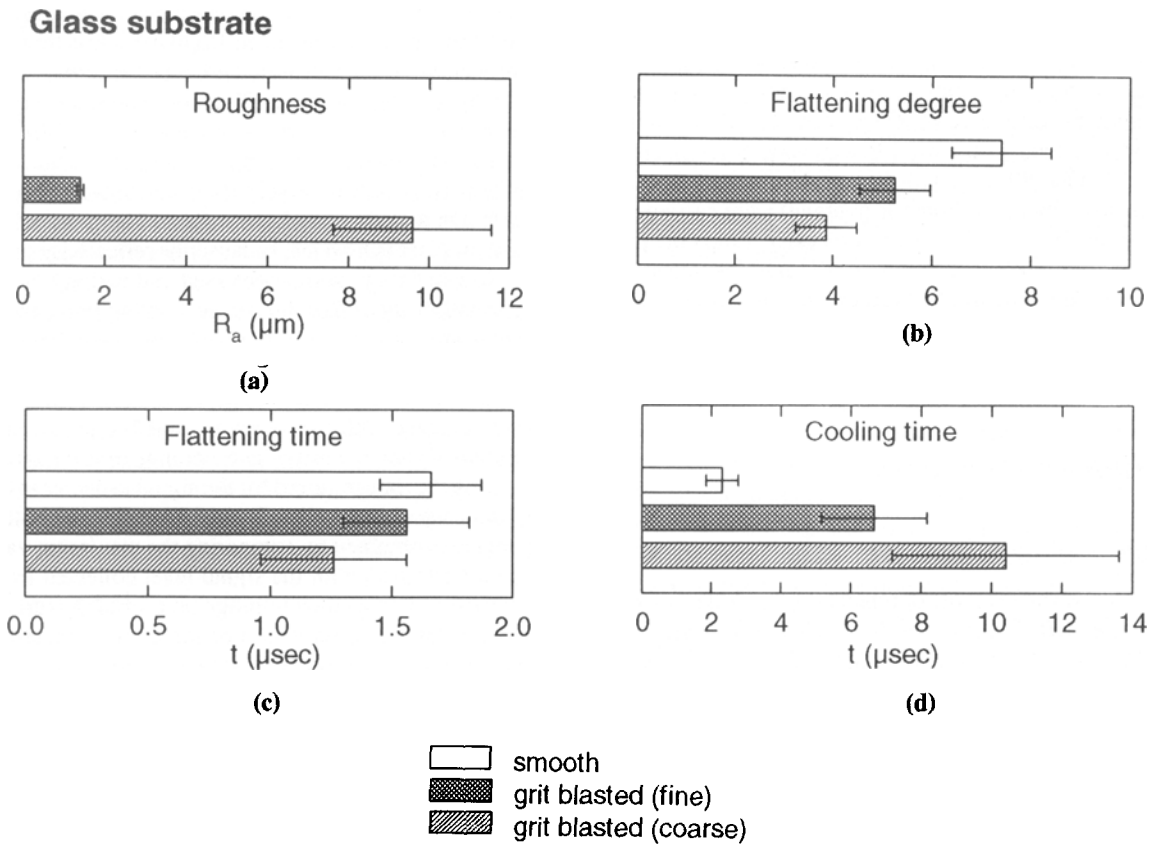

Fig. 5 *Surface roughness of the glass substrates (a) and the corresponding average flattening degree (b), flattening time (c), and cooling time (d). The roughness of the smooth substrate is 0.02 μm*

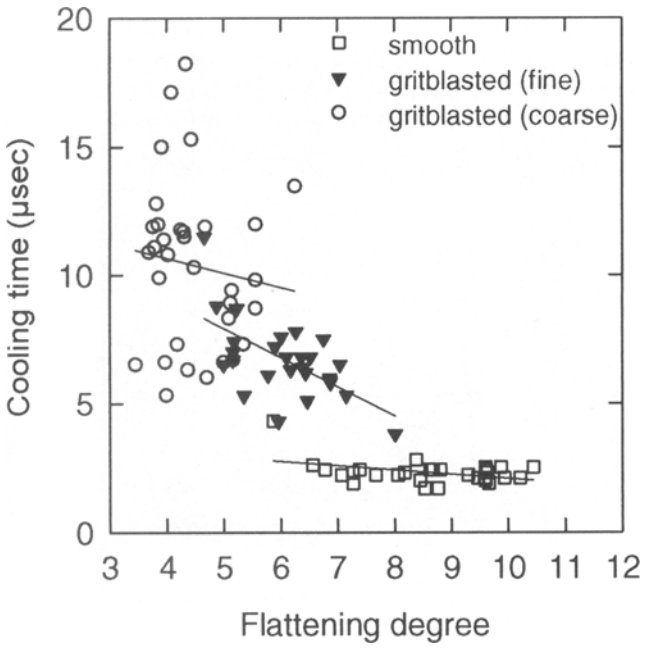

Fig. 6 Cooling time and flattening degree of individual impact events on smooth and grit-blasted glass substrates. Lines represent best fits through data collected on the different substrates

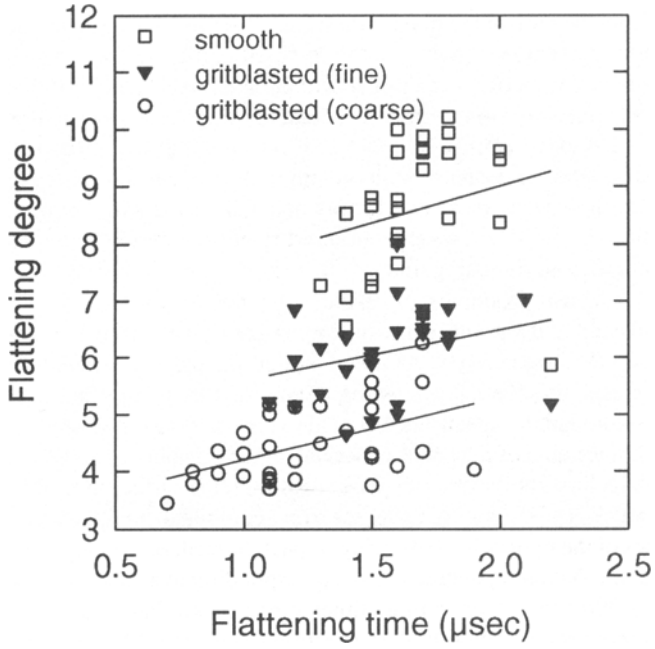

Fig. 7 Graphical representation of the flattening degree and flattening time of individual impact events on smooth and grit-blasted glass substrates. Lines represent best fits through data collected on the different substrates

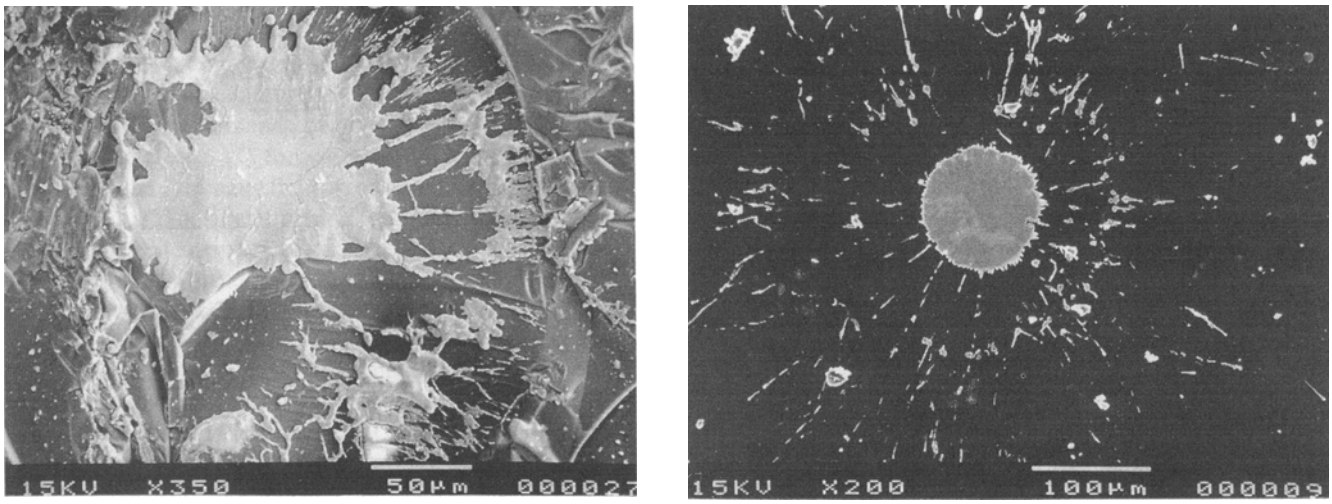

(a) (b)

Fig. 8 Electron micrographs of molybdenum splats on (a) a coarse grit-blasted glass substrate and (b) a smooth glass substrate

strate to 0.02 μm on the smooth surface. The flattening degree decreases from 7.4 on the smooth glass surface to 3.9 on the coarse grit-blasted surface. Estimations of the flattening degree based on the models discussed in Section 1 range from 6.0 for the Yoshiva model to 9.3 for the Madejski model. These values are obtained assuming a Reynolds number of 20,000 that corresponds to a 40 μm molybdenum particle, an impact velocity of 150 m/s, and a viscosity of 3×10^{-3} N · s/m^2, which is a typical value for molten metals near their melting point (Ref 18). Figure 5(c) also shows that the mean flattening time observed for coarse grit-blasted substrates is slightly shorter than for smooth substrates. On the other hand, surface preparation significantly influences the mean cooling time (Fig. 5d), which equals 10.4 μs for coarse grit-blasted substrates and 2.3 μs for smooth substrates.

As shown in Fig. 5, correlations exist among flattening degree, flattening time, and observed cooling time. These correlations are examined in more detail in Fig. 6 and 7. In Fig. 6, the cooling time for each individual particle is drawn as a function of the observed flattening degree. This latter factor is computed

from the ratio of the maximum signal observed during an impact to the average signal from the in-flight particles. Thus, part of the variation observed in the flattening degree on the different substrates results from the actual particle size distribution, which extends from 32 to 45 μm. As shown in Fig. 6, cooling time tends to decrease with flattening degree. Moreover, the relation between these two factors depends on the surface condition. Figure 7 shows the observed relation between flattening degree and flattening time.

Typical examples of splats collected on the coarse grit-blasted and smooth glass substrates are illustrated in Fig. 8(a) and (b), respectively. As noted earlier, for the grit-blasted substrates, the average flattening degree deduced from the maximum signal intensity is 3.9. This value is consistent with the surface area of the splats observed on the grit-blasted substrates (Fig. 8a). For the smooth glass substrates, the surface area of the splats is significantly lower than that computed from the analysis of the light collected during impact. Indeed, according to Fig. 5, the flattening degree is 7.4, corresponding to a splat diameter of 300 μm, which is three times greater than that actually observed on the smooth glass substrates (Fig. 8b). Moreover, the splat thickness is about 0.5 μm, as measured with an optical microscope using the sensitivity of the depth of field at high magnification. From these observations, it appears that only the central portion of the molybdenum splat adheres to the substrate surface after solidification and cooling. This portion represents less than 10% of the initial particle volume. Adhesion of this central portion is likely favored by the high pressure generated at the impact zone during particle flattening (Ref 19, 20). At the periphery of the splat, however, adhesion is insufficient to keep

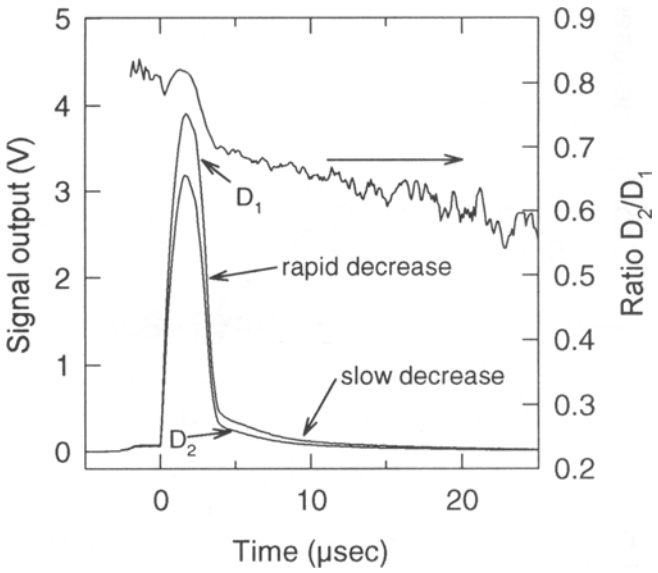

Fig. 9 Typical signals D_1 and D_2 collected during an impact on a smooth glass substrate. The corresponding ratio D_2/D_1 is also shown

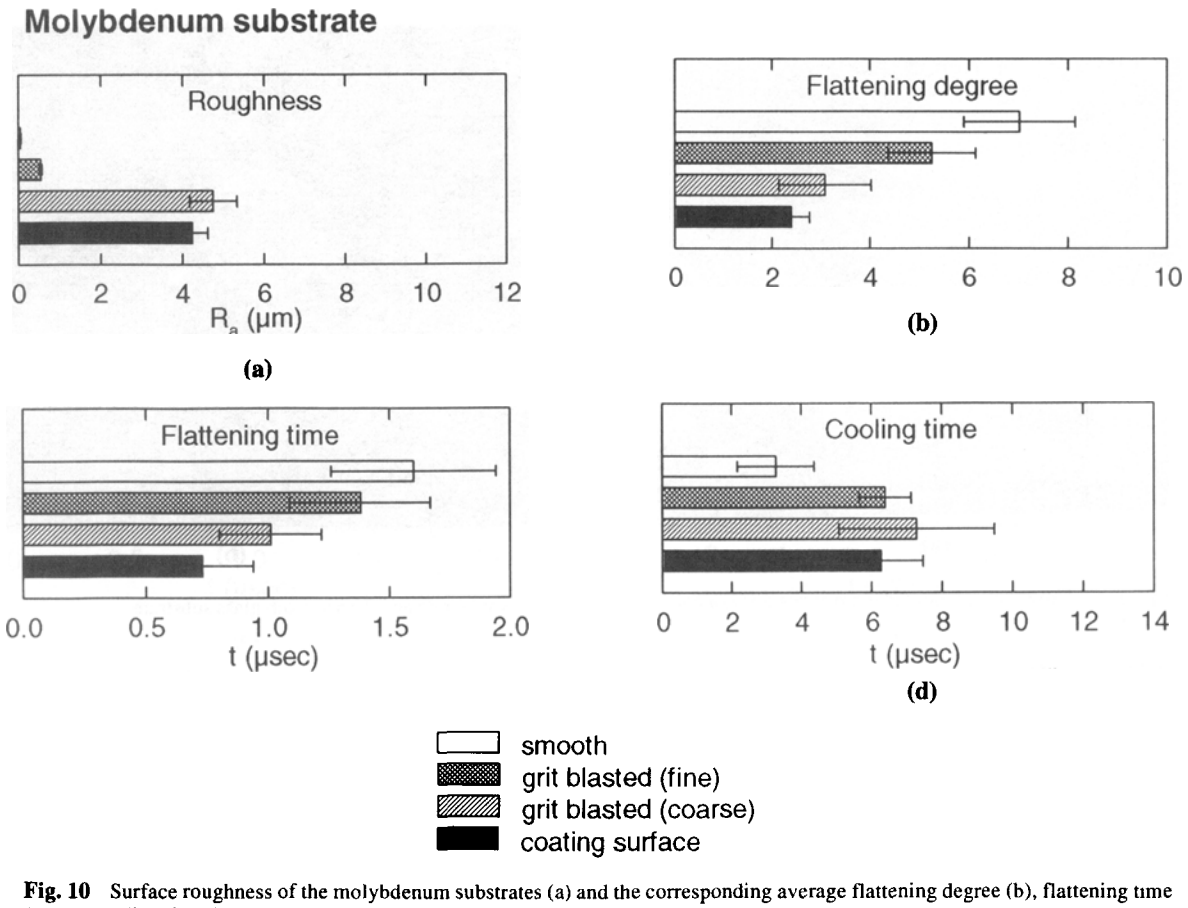

Fig. 10 Surface roughness of the molybdenum substrates (a) and the corresponding average flattening degree (b), flattening time (c), and cooling time (d)

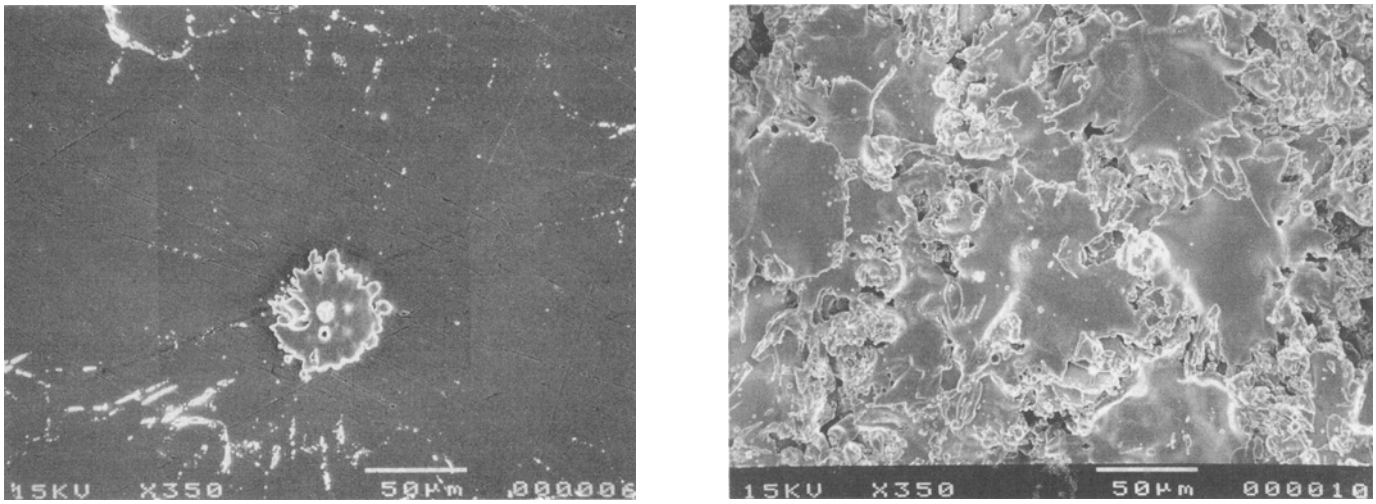

(a) (b)

Fig. 11 Electron micrographs of molybdenum splats on (a) a smooth molybdenum substrate and (b) the coating surface.

the material attached to the substrate, possibly due to the residual stress resulting from thermal contraction during cooling.

Typical signals collected during a particle impact on the smooth glass substrate are illustrated in Fig. 9. Signals D_1 and D_2 both drop rapidly after their maxima, leading to a very short cooling time, 2.3 µs on average (Fig. 5). After the initial rapid decrease, the signals continue to drop, but at a significantly lower rate. Three factors may be responsible for the observed rapid signal decrease: (1) formation of an annulus of molten metal exiting the pyrometer field of view a few microseconds after the impact, (2) splat contraction under the influence of surface tension, and (3) rapid cooling of the splat.

The potential influence of the first factor was investigated by monitoring impacts with a larger pyrometer field of view (1.4 by 2 mm). Signals collected in this new geometry were very similar to those shown in Fig. 9, but their intensities were relatively higher during the final slow decrease period. Because the time evolution of the signals up to the end of the rapid decrease period does not depend on the dimensions of the pyrometer field of view, this rapid decrease cannot be attributed to the exit of material from the pyrometer field of view after the particle impact.

The second factor concerns the possibility that the impinging molten particles may shrink under the influence of surface tension after reaching their maximum surface area about 2 µs after impact. Such shrinkage is illustrated for the case of mercury drops falling on a solid surface in Ref 17. The corresponding Reynolds number is about 28,000, comparable to the value associated with the impact of plasma-sprayed molybdenum particles as computed earlier. However, the influence of surface tension during flattening is less important in the latter case because the corresponding Weber number is about 4,000 compared to 140 in the former case. The larger the Weber number, the smaller the influence of surface tension during flattening (Ref 1, 2). However, the possibility that significant shrinkage of the molybdenum particles occurs before freezing cannot be totally excluded. Indeed, even if most of the initial kinetic energy is dissipated due to the viscosity of the molten metal (Ref 1-3), a significant decrease of the particle surface may occur in a short period of time in the case of particle segmentation (Ref 17).

Information about the influence of the third factor—rapid cooling of the splat—can be obtained from the evolution of the ratio D_2/D_1 as shown in Fig. 9. The rapid signal decrease is accompanied by a rapid drop in D_2/D_1, indicating a sharp temperature decrease during this period. It is thus likely that the observed rapid signal decrease results from rapid cooling of the splat. Shrinkage is less probable under these conditions, because the particle may rapidly freeze after reaching its maximum surface. On the coarse grit-blasted glass substrates, significant shrinkage does not intervene; the splat surface, as observed under the electron microscope, is comparable with that deduced from the maximum signal intensity during impact.

As mentioned previously, the intensities of signals D_1 and D_2 are relatively higher during the final slow decrease period when the larger pyrometer field of view is used. This indicates that a fraction of the material can exit the smaller pyrometer field of view (0.7 by 1 mm) and that this material, located in the periphery of the impact point, cools at a relatively slow rate.

3.3 *Impacts on Molybdenum*

Impacts on molybdenum polished and grit-blasted substrates are similar to those observed on the glass substrates (Fig. 10). The surface roughness (R_a) of the sprayed coatings and coarse grit-blasted substrates is nearly identical, but their surface topography is very different. Investigation of splat formation on the surface of sprayed coatings is important because it corresponds to the way the coatings are built. As observed on the glass substrates, the flattening degree tends to decrease with substrate

roughness. However, the flattening degree on the sprayed coatings is lower than that observed on the coarse grit-blasted substrates even if their surface roughness is slightly lower. This results from the particular topography of the sprayed coating surface. Moreover, the flattening degree on the molybdenum polished substrate is slightly lower than that on the smooth glass.

Typical shapes of the splats formed on the polished molybdenum substrate and coating surface are shown in Fig. 11. On the smooth surface (Fig. 11a), the splat surface area is significantly smaller than that computed from the maximum signal intensities, and small metal drops are visible at a relatively large distance from the point of impact. It is noteworthy that, during impact, a surface nearly equivalent to the entire region delimited by the string of small droplets was covered by the splat. On the coating surface, the observed splat area (Fig. 11b) was consistent with that computed from the maximum signal intensity.

As shown in Fig. 10, flattening time and flattening degree are correlated—that is, the higher the flattening degree, the longer the flattening time. Similar to impacts on glass, the shortest cooling time is reached on the smoother surface. Moreover, the increase in cooling time with surface roughness is lower than that observed for glass substrates. This is likely related to the higher thermal conductivity of molybdenum compared to glass and to a lower thermal resistance at the splat/substrate interface. The thermal conductivity of the substrate has less of an influence on the cooling of thin splats (0.5 μm). Indeed, in this case, the substrate heating during the splat cooling is limited because of the low total energy transfer.

In this work, the splat cooling time observed on the fine grit-blasted glass substrate is not significantly different from that on the molybdenum coating surface. These results are different from those reported in a previous study (Ref 11), where the cooling time was about three times longer on fine grit-blasted glass substrate. Moreover, in this earlier study, the flattening degree computed from the maximum signal intensity during impact was not significantly different on both surfaces. This was consistent with observations of splat thickness and diameter under optical and electron microscopes. Although the use of a coincidence technique to trigger the signal acquisition can produce biased results related to threshold adjustments, the observed differences between the results of these two studies are probably due to unlike particle conditions before impact. Indeed, as already discussed, particle diameter, velocity, and temperature prior to impact significantly influence the flattening process. It is expected, for example, that the influence of substrate roughness will be less when particles have lower temperature and velocity, because the flattening degree is reduced. In the limit case, surface roughness exerts no influence when the flattening degree is 1. This emphasizes the importance of developing more complete diagnostic techniques to determine in-flight particle parameters and to monitor subsequent impacts, as recently reported (Ref 8, 21).

4. Conclusion

The influence of surface roughness on the flattening and cooling of plasma-sprayed molybdenum particles was investigated. Information about flattening time, flattening degree, and cooling time was obtained by monitoring the thermal radiation emitted by the particles during impact. Substrate roughness significantly influences the degree of flattening and flattening time of the particles (i.e., the smoother the substrate, the larger the splat surface and the longer the flattening time). The observed flattening degrees on smooth substrates were consistent with those expected from theoretical and numerical models.

When impacts occurred on a smooth surface, the flattening degree was about 7, corresponding to a splat thickness of 0.5 μm. After impact, the rapid decrease of the thermal radiation emitted by these thin splats was attributed to a rapid temperature drop and a possible shrinkage of the splat under the influence of the molten metal surface tension. Moreover, the temperature of these splats was not radially uniform, with the cooling rate lower at the periphery. Finally, only a portion of the splats remained attached to the smooth substrate after cooling. When impacts occurred on rough surfaces, however, the area of the solidified splats was similar to that computed from the maximum signal intensity during impact.

References

1. J. Madejski, Solidification of Droplets on a Cold Surface, *Int. J. Heat Mass Transfer*, Vol 19,1976, p 1009-1013
2. J. Madejski, Droplets on Impact with a Solid Surface, *Int. J. Heat Mass Transfer*, Vol 26, 1983, p 1095-1098
3. G. Trapaga and J. Szekely, Mathematical Modeling of the Isothermal Impingement of Liquid Droplets in Spraying Processes, *Metall. Trans. B*, Vol 22B, 1991, p 901-914
4. T. Yoshida, T. Okada, H. Hideki, and H. Kumaoka, Integrated Fabrication Process for Solid Oxide Fuel Cells Using Novel Plasma Spraying, *Plasma Sources Sci. Technol.*, Vol 1, 1992, p 195-201
5. T. Watanabe, I. Kuribayashi, T. Honda, and A. Kanzawa, Deformation and Solidification of a Droplet on a Cold Substrate, *Chem. Eng. Sci.*, Vol 47, 1992, p 3059-3065
6. A. Vardelle, M. Vardelle, R. McPherson, and P. Fauchais, Study of the Influence of Particle Temperature and Velocity Distribution within a Plasma Jet on Coating Formation, *General Aspects of Thermal Spraying*, J.H. Zatt, Ed., Nederlands Instituut voor Lastechniek, The Hague, 1980, p 155-161
7. S.J. Yankee and B.J. Pletka, Effect of Plasma Spray Processing Variations on Particle Melting and Splat Spreading of Hydroxylapatite and Alumina, *J. Therm. Spray Technol.*, Vol 2, 1993, p 271-281
8. S. Fantassi, M. Vardelle, A. Vardelle, and P. Fauchais, Influence of the Velocity of Plasma Sprayed Particles on the Splat Formation, *Thermal Spray Coatings: Research, Design and Applications*, C.C. Berndt and T.F. Bernecki, Ed., ASM International, 1993, p. 1-6
9. B. Borgerding, H.J. Sölter, E. Lugscheider, and K. Simhan, Modelling of Temperature Gradients and Stress-Strain Distributions during the Plasma Spraying Process, *Powder Met. Int.*, Vol 24, 1993, p 240-245
10. D.J. Varacalle, Jr. and W.L. Riggs II, Analytically Modeling the Plasma Spray Deposition of Tribaloy 800, *Thermal Spray Coatings: Properties, Processes and Applications*, T.F. Bernecki, Ed., ASM International, 1992, p 245-250
11. C. Moreau, M. Lamontagne, and P. Cielo, Influence of the Coating Thickness on the Cooling Rates of Plasma-Sprayed Particles Impinging on a Substrate, *Surf. Coat. Technol.*, Vol 53, 1992, p 107-114
12. C. Moreau, P. Cielo, and M. Lamontagne, Flattening and Solidification of Thermally Sprayed Particles, *J. Therm. Spray Technol.*, Vol 1, 1992, p 317-323
13. C. Moreau, P. Cielo, M. Lamontagne, S. Dallaire, and M. Vardelle, Impacting Particle Temperature Monitoring during Plasma Spray Deposition, *Meas. Sci. Technol.*, Vol 1, 1990, p 807-814

14. R.E. Spjut, Transient Response of One- and Two-Color Optical Pyrometry, *Opt. Eng.*, Vol 26, 1987, p 467-472
15. J.-P. Hiernaut, R. Beukers, M. Hoch, T. Matsui, and R.W. Ohse, Determination of the Melting Point and of the Spectral and Total Emissivities of Tungsten, Tantalum, and Molybdenum in the Solid and Liquid States with a Six-Wavelength Pyrometer, *High Temp. High Press.*, Vol 18, 1986, p 627-633
16. P. Gougeon and C. Moreau, In-Flight Particle Surface Temperature Measurement: Influence of the Plasma Light Scattered by the Particles, *J. Therm. Spray Technol.*, Vol 2, 1993, p 229-234
17. A.M. Worthington, The Splash of a Drop and Allied Phenomena, *A Study of Splashes*, MacMillan, 1963, p 133-162
18. *Smithells Metals Reference Book*, 6th ed., E.A. Brandes, Ed., Butterworths, 1983, p 14-7 to 14-8
19. A.M. Shmakov and S.S. Ermakov, Impact Interaction of the Particle with the Substrate in Hot Gas Spraying, *Phys. Chem. Mater. Treat. (USSR)*, Vol 20, 1986, p 243-246
20. J.M. Houben, Future Developments in Thermal Spraying, *Second National Conference on Thermal Spray*, F.N. Longo, Ed., ASM International, 1984, p 1-19
21. M. Vardelle, A. Vardelle, P. Fauchais, and C. Moreau, Pyrometer System for Monitoring the Particle Impact on a Substrate during Plasma Spray Process, *Meas. Sci. Technol.*, Vol 5, 1994, p 205-212